

# Synthesis and Characterization of Lamellar and Hexagonal Mesostructured Aluminophosphates Using Alkyltrimethylammonium Cations as Structure-Directing Agents

Tatsuo Kimura,<sup>†</sup> Yoshiyuki Sugahara,<sup>†</sup> and Kazuyuki Kuroda<sup>\*,†,‡</sup>

Department of Applied Chemistry, Waseda University, Ohkubo-3, Shinjuku-ku, Tokyo 169-8555, Japan, and Kagami Memorial Laboratory for Materials Science and Technology, Waseda University, Nishiwaseda-2, Shinjuku-ku, Tokyo 169-0051, Japan

Received October 28, 1998. Revised Manuscript Received December 7, 1998

Lamellar and hexagonal mesostructured aluminophosphates (AIPOs) were prepared and characterized. The lamellar mesostructured AIPO (APW-1) formed hydrothermally and the condensed framework was composed of alternating  $\text{AlO}_4$  and  $\text{PO}_4$  units. The hexagonal mesostructured AIPO (APW-2) is formed by transformation of a layered precipitate composed of both aluminophosphate oligomers and alkyltrimethylammonium (ATMA) cations. Calcined APW-2 had a mesoporosity with the BET surface area of  $980 \text{ m}^2 \text{ g}^{-1}$  and a pore diameter of 1.8 nm after substantial shrinkage of the framework. Lamellar APW-1 formed under most of the conditions surveyed, while hexagonal APW-2 was obtained under very restricted conditions. In this system, the charge matching in the products is the most important factor, although the assemblies of ATMA cations are essential as the structure-directing agents.

## Introduction

Many kinds of microporous  $\text{AlPO}_4$ -*n* and  $\text{SAPO}$ -*n* materials have been synthesized,<sup>1</sup> and these materials have expanded the application of microporous inorganic solids to catalysts, catalyst supports, and adsorbents. Some of the materials, such as VPI-5<sup>2</sup> and JDF-20,<sup>3</sup> have large pore sizes of around 1.3 nm. Therefore, these materials have been expected to serve as novel and useful matrixes which allow larger molecules to enter in the pore system, although they are thermally unstable. Consequently, it is essential to overcome this problem by different approaches for the synthesis of large-pore  $\text{AlPO}_4$  materials.

After the discovery of mesoporous silicas prepared by using surfactant assemblies,<sup>4,5</sup> these synthetic methods have been applied to the synthesis of various mesoporous metal oxides.<sup>6–8</sup> Inorganic-surfactant mesostructured materials are precursors for the formation of mesoporous materials. However, they are also im-

portant as model systems for functional and biomimetic materials design, especially in phosphate-based materials.<sup>9</sup> The assembling ability of surfactants is effective for the formation of ordered mesostructured metal oxides with lamellar, hexagonal, and cubic phases.<sup>6</sup> Almost all of those reports involve the synthesis of simple oxides such as mesoporous silicas, and there have been no reports on the synthesis of mesoporous aluminophosphates until recently. One of the main difficulties would come from the organization of two different units on the surfactant assemblies. Here, we present the successful preparation of lamellar and hexagonal mesostructured aluminophosphates (AIPOs); the hexagonal AIPOs convert to mesoporous AIPOs by removal of surfactants. The synthesis and detailed characterization of these materials contribute to such fields as inorganic synthesis and materials chemistry including novel porous materials design.

Preparation of lamellar mesostructured aluminophosphates using surfactants has been reported by several research groups.<sup>10–16</sup> We have succeeded in synthesizing

\* To whom correspondence should be addressed.

<sup>†</sup> Department of Applied Chemistry.

<sup>‡</sup> Kagami Memorial Laboratory for Materials Science and Technology.

(1) (a) Wilson, S. T.; Lok, B. M.; Messina, C. A.; Cannan, T. R.; Flanigen, E. M. *J. Am. Chem. Soc.* **1982**, *104*, 1146–1147. (b) Lok, B. M.; Messina, C. A.; Patton, R. L.; Gajek, R. T.; Cannan, T. R.; Flanigen, E. M. *J. Am. Chem. Soc.* **1984**, *106*, 6092–6093.

(2) Davis, M. E.; Saldarriaga, C.; Montes, C.; Garces, J.; Crowder, C. *Nature* **1988**, *331*, 698–699.

(3) Huo, Q.; Xu, R.; Li, S.; Ma, Z.; Thomas, J. M.; Jones, R. H.; Chippindale, A. M. *J. Chem. Soc., Chem. Commun.* **1992**, 875–876.

(4) Yanagisawa, T.; Shimizu, T.; Kuroda, K.; Kato, C. *Bull. Chem. Soc. Jpn.* **1990**, *63*, 988–992.

(5) (a) Kresge, C. T.; Leonowicz, M. E.; Roth, W. J.; Vartuli, J. C.; Beck, J. S. *Nature* **1992**, *359*, 710–712. (b) Beck, J. S.; Vartuli, J. C.; Roth, W. J.; Leonowicz, M. E.; Kresge, C. T.; Schmitt, K. D.; Chu, C. T.-W.; Olson, D. H.; Sheppard, E. W.; McCullen, S. B.; Higgins, J. B.; Schlenker, J. L. *J. Am. Chem. Soc.* **1992**, *114*, 10834–10843.

(6) (a) Huo, Q.; Margolese, D. I.; Ciesla, U.; Feng, P.; Gler, T. E.; Sieger, P.; Leon, R.; Petroff, P. M.; Schüth, F.; Stucky, G. D. *Nature* **1994**, *368*, 317–321. (b) Huo, Q.; Margolese, D. I.; Ciesla, U.; Demuth, D. G.; Feng, P.; Gler, T. E.; Sieger, P.; Firouzi, A.; Chmelka, B. F.; Schüth, F.; Stucky, G. D. *Chem. Mater.* **1994**, *6*, 1176–1191.

(7) Behrens, P. *Angew. Chem., Int. Ed. Engl.* **1996**, *35*, 515–518.

(8) Sayari, A.; Liu, P. *Microporous Mater.* **1997**, *12*, 149–177.

(9) *Biomimetic Materials Chemistry*; Mann, S., Ed.; VCH Publishers: New York, 1996 and references therein.

(10) Czarnetzki, B. K.; Stork, W. H. J.; Dogterom, R. J. *Inorg. Chem.* **1993**, *32*, 5029–5033.

(11) Fyfe, C. A.; Schwieger, W.; Fu, G.; Kokotailo, G. T.; Grondy, H. *Symposium on Zeolites, Layered Compounds and Other Microporous Solids*, 209th National Meeting of the American Chemical Society, Anaheim, CA, Apr 2–7, 1995; American Chemical Society: Washington, DC, 1995; pp 266–268.

a hexagonal mesostructured  $\text{AlPO}_4^{17}$  by modifying the synthetic conditions for lamellar mesostructured aluminophosphates reported by Fyfe et al.<sup>11</sup> There are several reports on hexagonal mesostructured and mesoporous aluminophosphates,<sup>18–22</sup> and we also reported the successful formation of thermally stable mesoporous AlPOs using both surfactants with long alkyl chain lengths and solubilized organic molecules.<sup>23</sup> These materials had BET surface areas above  $700 \text{ m}^2 \text{ g}^{-1}$  and pore diameters in the range of 1.8–3.9 nm.

On the basis of our research on the mesostructured AlPOs,<sup>17,23</sup> we have noticed that the lamellar (APW-1) and hexagonal (APW-2) mesostructured AlPOs form under very closely interrelated synthetic conditions. Nevertheless, the frameworks were completely different between APW-1 and APW-2; APW-2 has never been found for other aluminophosphate materials.<sup>17,23</sup> On the basis of  $^{27}\text{Al}$  and  $^{31}\text{P}$  MAS NMR measurements, hexagonal mesostructured aluminophosphates reported recently by Luan et al. may possess similar frameworks to ours;<sup>20c</sup> however, the thermal stability (up to  $500 \text{ }^\circ\text{C}$ ) is lower than ours (up to  $600 \text{ }^\circ\text{C}$ , at the lowest). Therefore, in this paper, we investigate the structures of the APW-1 and APW-2, and we describe the formation conditions for APW-1 and APW-2 by changing the synthetic conditions. Moreover, the formation process of APW-2 is studied to understand the unique framework in more detail.

## Experimental Section

**1. Materials.** Hexadecyltrimethylammonium chloride ( $\text{C}_{16}\text{H}_{33}(\text{CH}_3)_3\text{NCl}$ ,  $\text{C}_{16}\text{TMACl}$ ), a tetramethylammonium hydroxide ( $(\text{CH}_3)_4\text{NOH}$ , TMAOH) aqueous solution (25 wt % in water), and aluminum triisopropoxide ( $\text{Al}(\text{O}^i\text{C}_3\text{H}_7)_3$ ,  $\text{Al}(\text{O}^i\text{Pr})_3$ ) were obtained from Tokyo Kasei Kogyo Co. Phosphoric acid (85%  $\text{H}_3\text{PO}_4$ ) was obtained from Kanto Chemical Co.

(12) Kimura, T.; Sugahara, Y.; Kuroda, K. *Phosphorus Res. Bull.* **1996**, *6*, 205–208.

(13) (a) Oliver, S.; Kuperman, A.; Coombs, N.; Lough, A.; Ozin, G. A. *Nature* **1995**, *378*, 47–50. (b) Oliver, S.; Coombs, N. G.; Ozin, G. A. *Adv. Mater.* **1995**, *7*, 931–935. (c) Ozin, G. A.; Oliver, S. *Adv. Mater.* **1995**, *7*, 943–947. (d) Oliver, S. R. J.; Ozin, G. A. *J. Mater. Chem.* **1998**, *8*, 1081–1085. (e) Oliver, S. R. J.; Lough, A. J.; Ozin, G. A. *Inorg. Chem.* **1998**, *37*, 5021–5028.

(14) (a) Chenite, A.; Page, Y. L.; Karra, V. R.; Sayari, A. *Chem. Commun.* **1996**, 411–412. (b) Sayari, A.; Karra, V. R.; Reddy, J. S.; Moudrakovski, I. L. *Chem. Commun.* **1996**, 413–414. (c) Sayari, A.; Moudrakovski, I.; Reddy, J. S. *Chem. Mater.* **1996**, *8*, 2080–2088.

(15) (a) Gao, Q.; Xu, R.; Chen, J.; Li, R.; Li, S.; Qiu, S.; Yue, Y. *J. Chem. Soc., Dalton Trans.* **1996**, 3303–3307. (b) Gao, Q.; Chen, J.; Xu, R.; Yue, Y. *Chem. Mater.* **1997**, *9*, 457–462.

(16) Pophal, C.; Schnell, R.; Fuess, H. *Stud. Surf. Sci. Catal.* **1997**, *105*, 101–108.

(17) (a) Kimura, T.; Sugahara, Y.; Kuroda, K. *Book of Abstracts*, 11th International Zeolite Conference, Seoul, Korea, Aug 12–17, 1996, RP 45. (b) Kimura, T.; Sugahara, Y.; Kuroda, K. *Chem. Lett.* **1997**, 983–984.

(18) Feng, P.; Xia, Y.; Feng, J.; Bu, X.; Stucky, G. D. *Chem. Commun.* **1997**, 949–950.

(19) (a) Chakraborty, B.; Pulikottil, A. C.; Das, S.; Viswanathan, B. *Chem. Commun.* **1997**, 911–912. (b) Chakraborty, B.; Pulikottil, A. C.; Viswanathan, B. *Appl. Catal.* **1998**, *167*, 173–181.

(20) (a) Zhao, D.; Luan, Z.; Kevan, L. *Chem. Commun.* **1997**, 1009–1010. (b) Zhao, D.; Luan, Z.; Kevan, L. *J. Phys. Chem.* **1997**, *101*, 6943–6948. (c) Luan, Z.; Zhao, D.; He, H.; Klinowski, J.; Kevan, L. *J. Phys. Chem.* **1998**, *102*, 1250–1259. (d) Luan, Z.; Zhao, D.; Levan, L. *Microporous Mesoporous Mater.* **1998**, *20*, 93–99.

(21) Holland, B. T.; Isbester, P. K.; Blanford, C. F.; Munson, E. J.; Stein, A. *J. Am. Chem. Soc.* **1997**, *119*, 6796–6803.

(22) Cheng, S.; Tzeng, J.-N.; Hsu, B.-Y. *Chem. Mater.* **1997**, *9*, 1788–1796.

(23) (a) Kimura, T.; Sugahara, Y.; Kuroda, K. *Chem. Commun.* **1998**, 559–560. (b) Kimura, T.; Sugahara, Y.; Kuroda, K. *Microporous Mesoporous Mater.* **1998**, *22*, 115–126.

**2. Synthesis of APW-1.** In a typical synthesis, 4.74 g of  $\text{C}_{16}\text{TMACl}$ , 10.79 g of 25 wt % TMAOH, 2.02 mL of 85%  $\text{H}_3\text{PO}_4$ , and 8.75 mL of water were mixed for several hours until a clear solution was obtained. Then, 3.07 g of  $\text{Al}(\text{O}^i\text{Pr})_3$  was added to this clear solution under vigorous stirring. After the mixture was stirred for 24 h, a wet gel was obtained, the composition of which was 0.5:1:1:2:65/ $\text{Al}_2\text{O}_3$ : $\text{P}_2\text{O}_5$ : $\text{C}_{16}\text{TMACl}$ :TMAOH: $\text{H}_2\text{O}$  and the pH was 8.5. The starting mixture was sealed and heated at  $130 \text{ }^\circ\text{C}$  for 5 days in a Teflon tube. The resultant solid product was washed with distilled water repeatedly and dried at  $80 \text{ }^\circ\text{C}$ .

**3. Synthesis of APW-2.** In a typical synthesis, a synthesis procedure was quite similar to that of APW-1. Only the amount of  $\text{Al}(\text{O}^i\text{Pr})_3$  was varied to 6.14 g. In this case, the formed mixture after being stirred for 24 h was a homogeneous solution like a thin milky lotion without solid phases. The composition of the formed mixture was 1:1:1:2:65/ $\text{Al}_2\text{O}_3$ : $\text{P}_2\text{O}_5$ : $\text{C}_{16}\text{TMACl}$ :TMAOH: $\text{H}_2\text{O}$  and the pH was 9.7. Even after the starting mixture was sealed and heated at  $130 \text{ }^\circ\text{C}$  for 5 days in a Teflon tube, a solid product was hardly obtained. The resultant liquid mixture was dispersed in distilled water with instant formation of a white solid. This solid was treated with distilled water repeatedly and dried at  $80 \text{ }^\circ\text{C}$ . When a lamellar mesostructured product formed slightly, the byproduct was removed by its slower sedimentation velocity.

**4. Variation in the Synthetic Conditions.** Several parameters such as the amount of water, the amount of TMAOH, the Al/P ratio in the starting mixtures were changed to determine the effect of the composition of the starting mixtures on the formation of mesostructured AlPOs. The reaction temperature and the reaction time were also varied. The composition of the starting mixtures was described as  $x:1:1:y:z/\text{Al}_2\text{O}_3$ : $\text{P}_2\text{O}_5$ : $\text{C}_{16}\text{TMACl}$ : $y$ TMAOH: $z$  $\text{H}_2\text{O}$ , where  $x$  was 0.3–1.2,  $y$  was 0–2.4, and  $z$  was 40–400. The synthesis procedure was quite similar to that of APW-1. After the mixtures (liquids and solids), which were obtained after heating at  $130 \text{ }^\circ\text{C}$  for 5 days, were dispersed in distilled water, the products were recovered by centrifuging.

**5. Characterization.** Powder X-ray diffraction (XRD) patterns were obtained by using a Mac Science MXP<sup>3</sup> diffractometer with monochromated  $\text{CuK}\alpha$  radiation and a M03XHF<sup>22</sup> diffractometer with monochromated  $\text{FeK}\alpha$  radiation. FT-IR spectra were recorded on a Perkin-Elmer FTIR-1640. Transmission electron micrographs (TEMs) were taken by a HITACHI H-8100A electron micrograph, operated at 200 kV. Solid-state  $^{27}\text{Al}$  MAS NMR measurement was performed on a JEOL GSX-400 spectrometer at a spinning rate of 3.5 kHz and a resonance frequency of 104.05 MHz with a  $45^\circ$  pulse length of  $4.4 \mu\text{s}$  and a recycle time of 5 s. Solid-state  $^{31}\text{P}$  MAS NMR was performed at a spinning rate of 5 kHz and a resonance frequency of 161.70 MHz with a  $60^\circ$  pulse length of  $5 \mu\text{s}$  and a recycle time of 20 s. Solid-state  $^{13}\text{C}$  CP/MAS NMR was performed at a spinning rate of 3.5 kHz and a resonance frequency of 100.40 MHz with a pulse length of  $5.1 \mu\text{s}$  and a recycle time of 5 s. The chemical shifts were quoted from  $\text{Al}(\text{H}_2\text{O})_6^{3+}$  of 0 ppm,  $\text{P}(\text{C}_6\text{H}_5)_3$  of  $-8.4$  ppm, and adamantane of 29.5 ppm, respectively.  $^{27}\text{Al}$  and  $^{31}\text{P}$  NMR measurements of the starting mixtures were performed on a JEOL EX-270 spectrometer at resonance frequencies of 70.26 and 109.25 MHz with  $90^\circ$  pulse lengths of 9.6 and  $5.2 \mu\text{s}$  and recycle times of 1.0 and 1.2 s, respectively. The chemical shifts were quoted from  $\text{Al}(\text{H}_2\text{O})_6^{3+}$  of 0 ppm and 85%  $\text{H}_3\text{PO}_4$  of 0 ppm, respectively. The Al/P ratios of the products were measured by ICP (Jarrell ash ICAP575 Mark II) and the amounts of organic fractions in the products were determined by CHN analysis (Perkin-Elmer PE-2400II). Nitrogen adsorption isotherms were obtained by a BELSORP 28 (Bel Japan, Inc.) at 77 K. The samples were preheated at  $120 \text{ }^\circ\text{C}$  for 3 h under vacuum.

## Results

**1. Characteristics of APW-1.** The XRD pattern of APW-1 shows the main peak at a  $d$ -spacing of 3.1 nm and peaks of higher order reflections were observed at

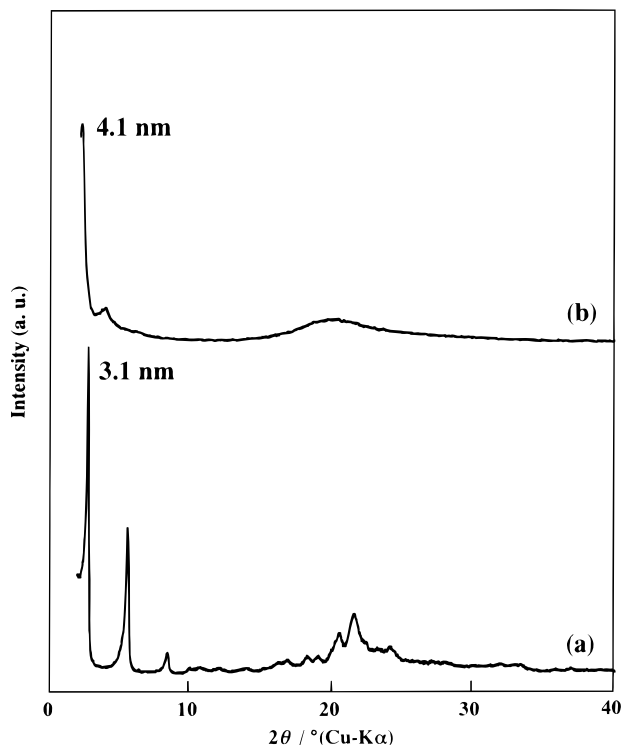


Figure 1. XRD patterns of (a) APW-1 and (b) APW-2.

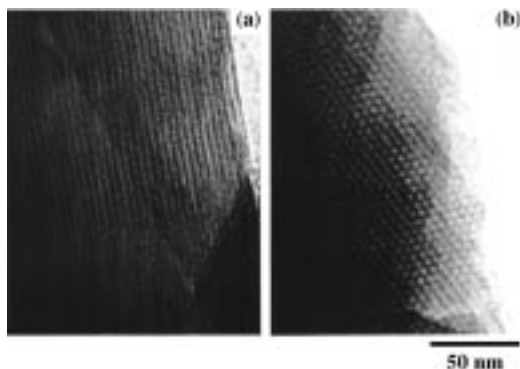


Figure 2. TEM images of (a) APW-1 and (b) APW-2.

low diffraction angles (Figure 1a). The TEM image of APW-1 in Figure 2a reveals that clear striped patterns were observed and the repeat distance of the striped patterns was 3.1 nm, being in good agreement with the  $d$ -spacing recorded by XRD. In addition, the  $d$ -spacing of APW-1 changed from 3.1 to 4.5 nm by swelling in  $n$ -decyl alcohol. Moreover, APW-1 was thermally unstable above 200 °C. These results indicate that APW-1 is a lamellar mesostructured AIPO.

The XRD pattern of APW-1 shows several peaks in the  $2\theta$  region higher than 15°. These peaks cannot be assigned to tridymite-like and cristobalite-like AIPO<sub>4</sub> and AIPO<sub>4</sub>-20 which could possibly form under the synthetic conditions. The scanning electron micrograph (SEM) of APW-1 showed the presence of platelet crystals of 1–10  $\mu\text{m}$  in size without other phases. These results suggest that the XRD peaks observed above 15° are due to the structure of APW-1. The FT-IR spectrum of APW-1 showed several peaks in the region of 1400–400  $\text{cm}^{-1}$ . The peak at 1228  $\text{cm}^{-1}$  is similar to those observed for VPI-5 and AIPO<sub>4</sub>-5 which have both four- and six-membered rings composed of tetrahedral TO<sub>4</sub>

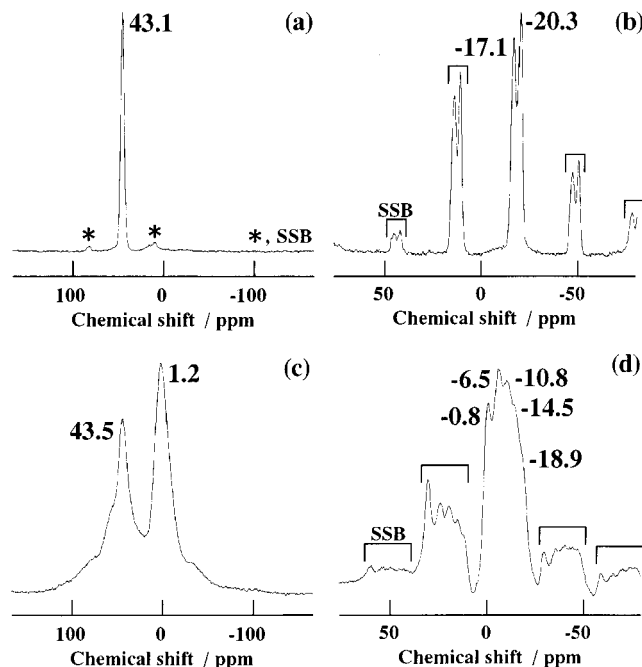


Figure 3. (a) <sup>27</sup>Al and (b) <sup>31</sup>P MAS NMR spectra of APW-1 and (c) <sup>27</sup>Al and (d) <sup>31</sup>P MAS NMR spectra of APW-2.

units (T; Al or P).<sup>24</sup> Several peaks in the region of 1200–1000  $\text{cm}^{-1}$ , 780–600  $\text{cm}^{-1}$ , and 500–400  $\text{cm}^{-1}$  are due to the asymmetric stretching of Al–O–P, the symmetric stretching of Al–O–P, and the bending of O–T–O, respectively.<sup>24</sup>

The <sup>27</sup>Al and <sup>31</sup>P MAS NMR spectra of APW-1 are shown in Figure 3a,b. The <sup>27</sup>Al MAS NMR spectrum showed a sharp signal at 43.1 ppm, indicating the presence of four-coordinated Al which can be assigned to Al(OP)<sub>4</sub> units.<sup>10,12,25</sup> The conclusion that alumina impurity does not exist in the product is supported by the absence of any peaks due to six-coordinated Al. The <sup>31</sup>P MAS NMR spectrum showed two peaks, at –17.1 and –20.3 ppm, both of which are assignable to –OP(OAl)<sub>3</sub> units.<sup>10,12</sup> The composition of APW-1 was 2.40:1:0.93/C<sub>16</sub>TMA:Al<sub>3</sub>P<sub>4</sub>O<sub>16</sub>:H<sub>2</sub>O. The NMR study and the chemical analysis indicate that APW-1 has a framework composed of alternating AlO<sub>4</sub> and PO<sub>4</sub> units.

**2. Characteristics of APW-2.** The XRD pattern of APW-2 (Figure 1b) shows the main peak at a  $d$ -spacing of 4.1 nm. From the XRD peaks (Figure 4a), the peaks of 4.1, 2.4, and 2.1 nm are assignable to the (100), (110), and (200) reflections of a hexagonal phase, respectively. The TEM image of APW-2 (Figure 2b) shows a relatively ordered hexagonal arrangement. The periodic distance of adjacent pores was  $\approx 4.0$  nm, which is smaller than the lattice parameter (4.8 nm). We think that the periodic distance might be decreased during the TEM measurement because condensation of a less condensed framework might occur by electron beam irradiation under the very high vacuum conditions.

The XRD pattern of APW-2 in the  $2\theta$  region above 15° was analogous to that of MCM-41.<sup>26</sup> The FT-IR

(24) Davis, M. E.; Montes, C.; Hathaway, P. E.; Arhancet, J. P.; Hasha, D. L.; Garces, J. M. *J. Am. Chem. Soc.* **1989**, *111*, 3919–3924.

(25) Müller, D.; Jahn, E.; Ladwig, G.; Haubenreisser, U. *Chem. Phys. Lett.* **1984**, *109*, 332–336.

(26) Beck, J. S.; Vartuli, J. C.; Kennedy, G. J.; Kresge, C. T.; Roth, W. J.; Schramm, S. E. *Chem. Mater.* **1994**, *6*, 1816–1821.

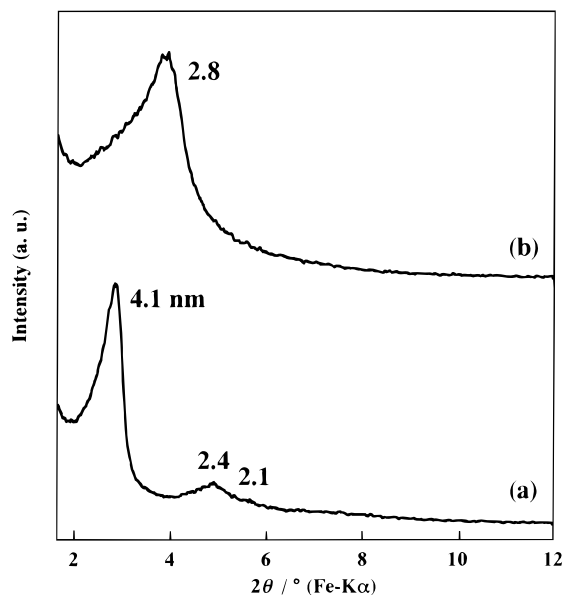


**Figure 4.** XRD patterns of (a) APW-2 and (b) APW-2 calcined at 600 °C.

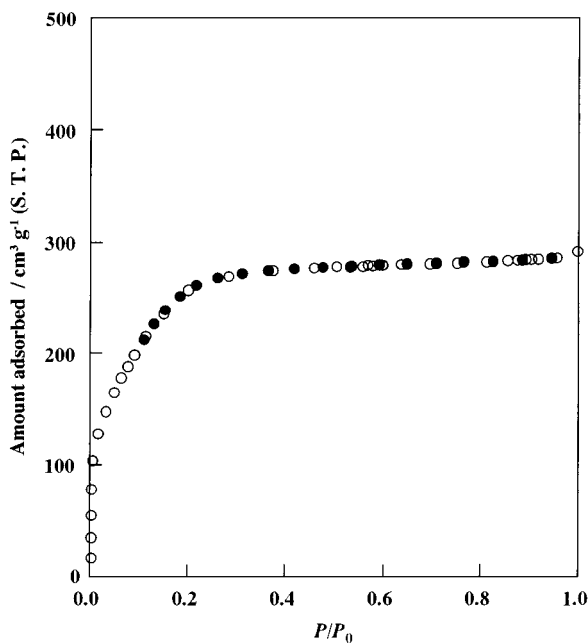


**Figure 5.** N<sub>2</sub> isotherm of APW-2 calcined at 600 °C. Filled symbol denotes desorption.

spectrum of APW-2 showed broad peaks in the region of 1400–400 cm<sup>-1</sup>, being different from those observed in APW-1. The peaks in the region of 1400–1000 cm<sup>-1</sup> due to the asymmetric stretching of Al–O–P, 780–600 cm<sup>-1</sup> due to the symmetric stretching of Al–O–P, and 500–400 cm<sup>-1</sup> due to the bending of O–T–O were very broad. The peak due to O–T–O bending was relatively small.

The <sup>27</sup>Al MAS NMR spectrum (Figure 3c) indicated the presence of both four- and six-coordinated Al, observed at 43.5 and 1.2 ppm, respectively. Four-coordinated Al can be assigned to Al(OP)<sub>4</sub> and/or Al(OP)<sub>4-x</sub>(OH)<sub>x</sub> based on the chemical shift and the asymmetric profile.<sup>10–12,16</sup> The signal due to six-coordinated Al disappeared after calcination at 600 °C (Figure 6a). Therefore, the six-coordinated Al may be coordinated with not only PO<sub>4</sub> units but also water molecules.

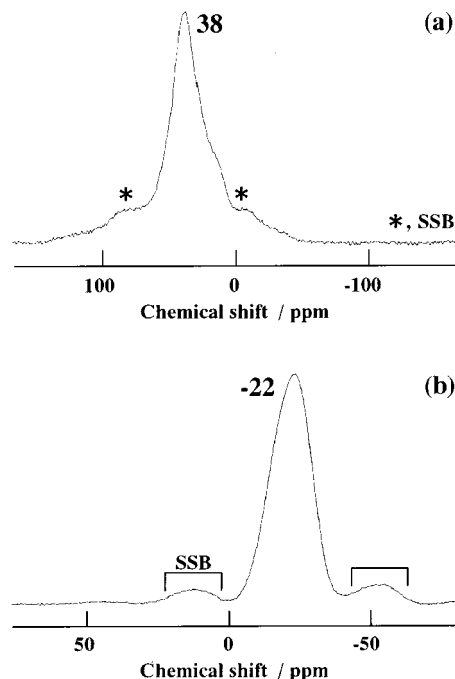


**Figure 6.** (a) <sup>27</sup>Al and (b) <sup>31</sup>P MAS NMR spectra of APW-2 calcined at 600 °C.

The <sup>31</sup>P MAS NMR spectrum (Figure 3d) shows that several peaks were observed in the range from 0 to –20 ppm, mainly observed in the range from –6 to –15 ppm. Mortlock et al. reported that boldface P atoms in Al(H<sub>2</sub>O)<sub>5</sub>(H<sub>2</sub>PO<sub>4</sub>), Al(H<sub>2</sub>O)<sub>4</sub>(H<sub>2</sub>PO<sub>4</sub>)<sub>2</sub>, and Al(H<sub>2</sub>O)<sub>4</sub>(H<sub>3</sub>PO<sub>4</sub>)(H<sub>2</sub>PO<sub>4</sub>) are observed at –9.5 ppm, that P atoms in Al(H<sub>2</sub>O)<sub>5</sub>(H<sub>3</sub>PO<sub>4</sub>), Al(H<sub>2</sub>O)<sub>4</sub>(H<sub>3</sub>PO<sub>4</sub>)<sub>2</sub>, and Al(H<sub>2</sub>O)<sub>4</sub>(H<sub>3</sub>PO<sub>4</sub>)(H<sub>2</sub>PO<sub>4</sub>) are observed at –12.6 ppm, and that P atoms in (HO)<sub>2</sub>P{OAl(H<sub>2</sub>O)<sub>5</sub>}<sub>2</sub> are observed at –16.5 ppm.<sup>27</sup> In the spectrum of APW-1 described above, <sup>-</sup>OP(OAl)<sub>3</sub> units are observed at –17.1 and –20.3 ppm. In addition, the signals due to P(OAl)<sub>4</sub> units of microporous crystalline AlPO<sub>4-n</sub> and SAPO-n materials are observed in the range from –19 to –31 ppm.<sup>28</sup> On the basis of these reports, the signals in the <sup>31</sup>P MAS NMR spectrum of APW-2 are assigned by the idea that the chemical shifts of P atoms change toward higher magnetic fields with the number of Al atoms bonded to PO<sub>4</sub> units. Consequently, the PO<sub>4</sub> units in APW-2 are mainly bonded to one or two Al atoms, meaning that APW-2 has a less condensed framework. The composition of APW-2 was 2.48:3:2:1.42/C<sub>16</sub>TMA:Al<sub>2</sub>O<sub>3</sub>:P<sub>2</sub>O<sub>5</sub>:H<sub>2</sub>O; the Al/P ratio was 1.49, being different from unity which should be expected from an ideal three-dimensional AlPO<sub>4-n</sub>.<sup>1</sup> This may be related to the incomplete condensation of PO<sub>4</sub> units and the presence of six-coordinated Al coordinated to some water molecules.

APW-2 was calcined at 600 °C for 1 h in flowing N<sub>2</sub>, and for 1 h in flowing air to remove the organic fractions. Figure 4 shows that the main peak at the *d*-spacing of 4.1 nm shifted to 2.8 nm and only one peak was observed after calcination, indicating that the size and the regularity of the hexagonal arrays became lower

(27) (a) Mortlock, R. F.; Bell, A. T.; Radke, C. J. *J. Phys. Chem.* **1993**, *97*, 775–782. (b) Mortlock, R. F.; Bell, A. T.; Radke, C. J. *J. Phys. Chem.* **1993**, *97*, 767–774.

(28) Blackwell, C. S.; Patton, R. L. *J. Phys. Chem.* **1984**, *88*, 6135–6139.

by calcination. The N<sub>2</sub> isotherm of calcined APW-2 shown in Figure 5 was intermediate between types I and IV. The BET surface area and the pore volume were 980 m<sup>2</sup> g<sup>-1</sup> and 0.44 mL g<sup>-1</sup>, respectively. The average pore diameter calculated by the Horváth–Kawazoe method<sup>29</sup> was ≈1.8 nm. Although the presence of an amorphous phase cannot be denied, the main phase is mesoporous AlPO because the BET surface area and the pore volume are similar or just slightly lower than those observed in mesoporous silicas.

The <sup>27</sup>Al and <sup>31</sup>P MAS NMR spectra of calcined APW-2 are shown in Figure 6. The <sup>27</sup>Al MAS NMR spectrum shows that only four-coordinated Al was observed at 38 ppm, strongly suggesting that the Al<sup>IV</sup>O<sub>4</sub> unit is surrounded by mainly P.<sup>23,30</sup> Although the Al/P ratio (≈1.5) might suggest the presence of Al–O–Al bonds, such bonds are unlikely, judging from very different chemical shifts due to [Al<sup>IV</sup>O<sub>4</sub>(nAl)] (n = 1–4).<sup>30</sup> The <sup>31</sup>P MAS NMR spectrum showed the broad peak centered at –22 ppm, indicating the progress of condensation of the framework by calcination.<sup>23,27,28</sup> This phenomenon can explain the structural change of APW-2 to porous AlPO with lower regularity during calcination.

### 3. Investigation of the Synthetic Conditions.

Lamellar APW-1 had a relatively condensed framework and hexagonal APW-2 had a less condensed framework. Therefore, it is considered that the control of the framework structures is the most important for the synthesis of APW-1 and APW-2. In this section, the effect of the synthetic conditions on the formation of mesostructured AlPOs was studied by varying the parameters.

**3.1. Effect of the Amount of TMAOH.** The composition of the starting mixtures was changed as follows: 1:1:1:y:65/Al<sub>2</sub>O<sub>3</sub>:P<sub>2</sub>O<sub>5</sub>:C<sub>16</sub>TMACl:TMAOH:H<sub>2</sub>O, where y was varied from 0 to 2.8. The XRD patterns of the products are shown in Figure 7. No mesostructured products formed under the TMAOH-free conditions, while mesostructured products were obtained by adding TMAOH (y ≥ 0.8). With an increase in the amount of TMAOH, the structure of the products changed from lamellar to hexagonal. When the pH values of the starting mixtures were around 10 (y = 1.8–2.2) (Table 1), hexagonal mesostructured products were obtained as the main product. The Al/P ratios of the products (Table 1) increased with an increase in the amount of TMAOH. Hexagonal mesostructured products had Al/P ratios around 1.5. Because no TMA cations were detected in all the mesostructured products by <sup>13</sup>C CP/MAS NMR measurement, TMAOH acts as a basic source to adjust the pH values of the starting mixtures. When a large amount of TMAOH was added (y = 2.4), the XRD peaks were broadened and the Al/P ratio suddenly became very high. In this case, a notable amount of six-coordinated Al was present in the product as an impurity because the <sup>27</sup>Al MAS NMR spectrum of the calcined product showed the presence of six-coordinated Al. Thus, the formation of APW-1 and APW-2 without an alumina impurity can be achieved by the suitable addition of TMAOH.

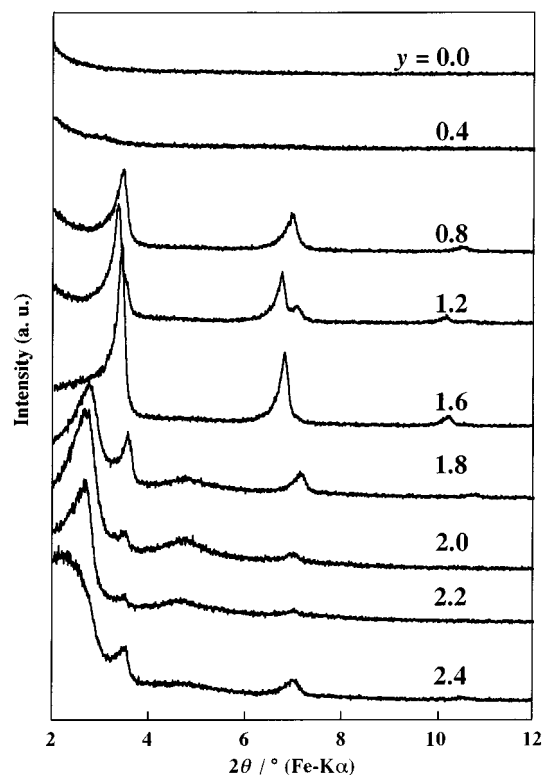


**Figure 7.** XRD patterns of the products obtained from a starting mixture with the composition 1:1:1:y/Al<sub>2</sub>O<sub>3</sub>:P<sub>2</sub>O<sub>5</sub>:C<sub>16</sub>TMACl:TMAOH:H<sub>2</sub>O, where y was varied in the range from 0 to 2.4.

**Table 1.** Effect of Composition of Starting Mixtures on Al/P Ratio of Obtained Products<sup>a</sup>

Al <sub>2</sub> O <sub>3</sub> molar ratio (x)	TMAOH molar ratio (y)	pH value of starting mixture	Al/P ratio of obtained product
1.0	0.0	3.4	0.99
	0.4	5.7	1.08
	0.8	6.9	1.08
	1.2	7.4	1.10
	1.6	8.8	1.19
	1.8	9.2	1.43
	2.0	9.7	1.52
	2.2	10.5	1.62
	2.4	11.6	2.23
0.3			0.86
0.5		8.5	0.79
0.7	2.0	8.6	1.03
0.85		9.6	1.29
1.0		9.7	1.52

<sup>a</sup> The composition of the starting mixture was x:1:1:y:65/Al<sub>2</sub>O<sub>3</sub>:P<sub>2</sub>O<sub>5</sub>:C<sub>16</sub>TMACl:TMAOH:H<sub>2</sub>O, where x was varied from 0.3 to 1.2 and y was varied from 0 to 2.4.

The states of the starting mixtures changed from wet gels (y ≤ 1.8) to thin milky solutions (y = 1.8–2.2), and to a clear solution (y = 2.4) with an increase in the amount of TMAOH. This observation agrees well with the change from aluminophosphate gels to clear solutions at around pH = 10 under when Al/P = 1, reported by Mortlock et al.<sup>27a</sup> The amount of TMAOH affects the solubility of the Al sources and/or aluminophosphate species in the starting mixtures.

**3.2. Effect of the Amount of Water.** The composition of the starting mixtures was changed as follows: 1:1:1:z/Al<sub>2</sub>O<sub>3</sub>:P<sub>2</sub>O<sub>5</sub>:C<sub>16</sub>TMACl:TMAOH:H<sub>2</sub>O, where z was varied from 40 to 400. The XRD patterns of the

(29) Horváth, G.; Kawazoe, K. *J. Chem. Eng. Jpn.* **1983**, *16*, 470–475.

(30) Müller, D.; Gessner, W.; Samoson, A.; Lippmaa, E.; Scheler, G. *J. Chem. Soc., Dalton Trans.* **1986**, 1277–1281.

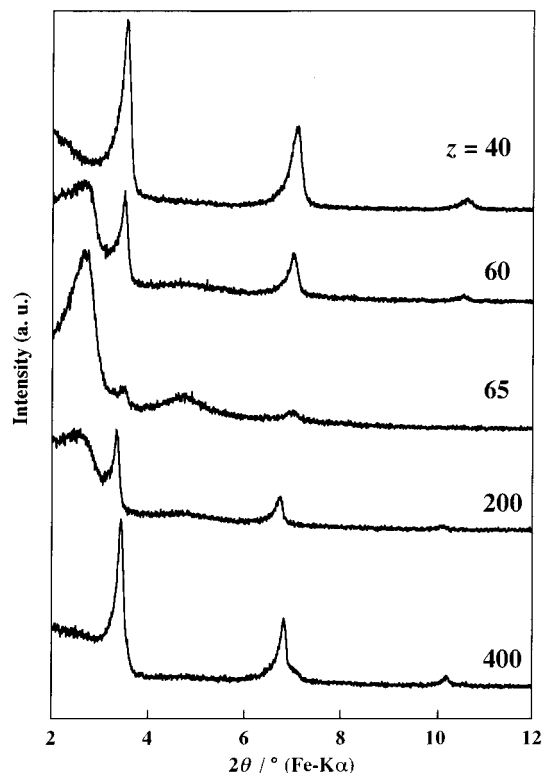


**Figure 8.** XRD patterns of the products obtained from a starting mixture with the composition 1:1:2:z/Al<sub>2</sub>O<sub>3</sub>:P<sub>2</sub>O<sub>5</sub>:C<sub>16</sub>TMACl:TMAOH:H<sub>2</sub>O, where z was varied in the range from 40 to 400.

products are shown in Figure 8. A hexagonal mesostructured product formed at  $z = 65$ . With the increase and decrease in the amount of water, lamellar mesostructured products formed. In addition, when the amount of water was slightly changed, a lamellar mesostructured product largely formed as a byproduct ( $z = 60$ ). When the amount of water was varied in the region of 40, 60, 65, 200, and 400, the pH values of the starting mixtures were correspondingly changed in the region of 10.3, 10.4, 9.7, 8.5, and 7.8, respectively. The reason for the formation of lamellar mesostructured products at both higher and lower pH values is not clear. Nevertheless, the formation at lower pH values is similar to the findings in section 3.1 ( $y = 1.2$ – $1.6$ ).

The pH values of the starting mixtures were almost the same (10.3–10.4) under the conditions of a small amount of water. Although hexagonal mesostructured products formed at around pH = 10 (section 3.1), lamellar mesostructured products were obtained ( $z = 40$ ). In the <sup>27</sup>Al NMR spectrum of the starting mixture with  $z = 40$ , a small amount of four-coordinated Al was observed at  $\approx 47$  ppm, although most of the Al species were present as six-coordinated Al at  $\approx 0$  ppm. When a slight amount of tetraethoxysilane was added (Si/P = 0.05) under the optimal conditions for APW-2, a lamellar mesostructured product formed; four-coordinated Al was not observed in the starting mixture with  $z = 65$ . These results suggest that the coexistence of four-coordinated species in the starting mixtures leads to the formation of APW-1.

**3.3. Effect of the Al/P Ratio.** The composition of the starting mixtures was changed as follows:  $x$ :1:1:2:65/Al<sub>2</sub>O<sub>3</sub>:P<sub>2</sub>O<sub>5</sub>:C<sub>16</sub>TMACl:TMAOH:H<sub>2</sub>O, where  $x$  was varied from 0.3 to 1.2. The XRD patterns of the products

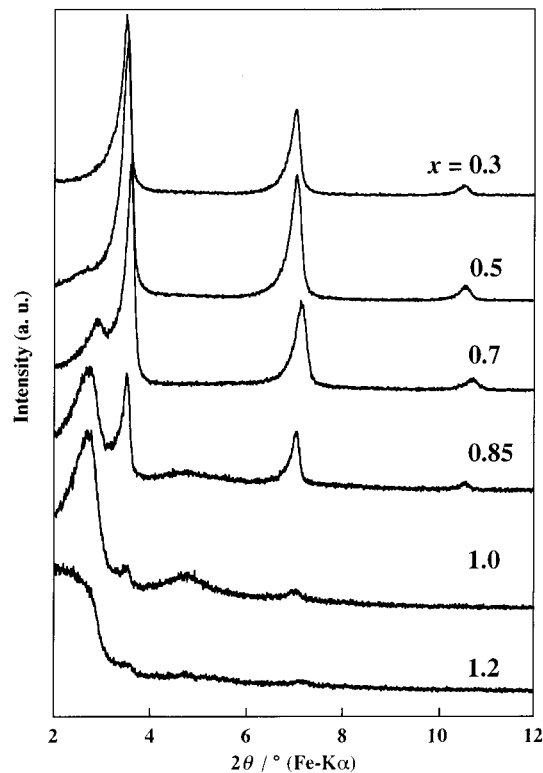


**Figure 9.** XRD patterns of the products obtained from a starting mixture with the composition  $x$ :1:1:2:65/Al<sub>2</sub>O<sub>3</sub>:P<sub>2</sub>O<sub>5</sub>:C<sub>16</sub>TMACl:TMAOH:H<sub>2</sub>O, where  $x$  was varied in the range from 0.3 to 1.2.

are shown in Figure 9. When the Al/P ratios of the starting mixtures were lower than 1, lamellar mesostructured products were obtained as main products. The pH values of the starting mixtures and the Al/P ratios of the products shown in Table 1 became higher with an increase in the amount of Al(O'Pr)<sub>3</sub>. The relation between the variation in the pH values and the structural change of the obtained products is in good agreement with the results observed for a variation in the amount of TMAOH.

Because the pH values varied correspondingly with a variation in the amount of Al(O'Pr)<sub>3</sub>, starting mixtures with different Al/P ratios were prepared by adding TMAOH to eliminate the effect of pH. The pH values of the following starting mixtures were around 10. By using a starting mixture with a composition of 0.7:1:1:2.4:65/Al<sub>2</sub>O<sub>3</sub>:P<sub>2</sub>O<sub>5</sub>:C<sub>16</sub>TMACl:TMAOH:H<sub>2</sub>O, a hexagonal mesostructured product was obtained. However, a lamellar mesostructured product was obtained by using a composition of 0.3:1:1:2.8:65/Al<sub>2</sub>O<sub>3</sub>:P<sub>2</sub>O<sub>5</sub>:C<sub>16</sub>TMACl:TMAOH:H<sub>2</sub>O. Even when the same pH conditions were used, a lamellar mesostructured product formed with a heavily deviated Al/P ratio. Mortlock et al. reported that four-coordinated Al species in aqueous solutions containing Al<sup>3+</sup>, PO<sub>4</sub><sup>3-</sup>, and TMAOH are present in the cases of lower Al/P ratios.<sup>27a</sup> In our experiments with lower Al/P ratios, four-coordinated Al species lead to the formation of lamellar APW-1, described in section 3.2. On the other hand, APW-2 can be obtained under the conditions of restricted molar ratios of (0.7–1.0):1:1:(2.0–2.4):65/Al<sub>2</sub>O<sub>3</sub>:P<sub>2</sub>O<sub>5</sub>:C<sub>16</sub>TMACl:TMAOH:H<sub>2</sub>O at 130 °C without the formation of APW-1. Because the pH value, the Al/P ratio, and the amount of water of the

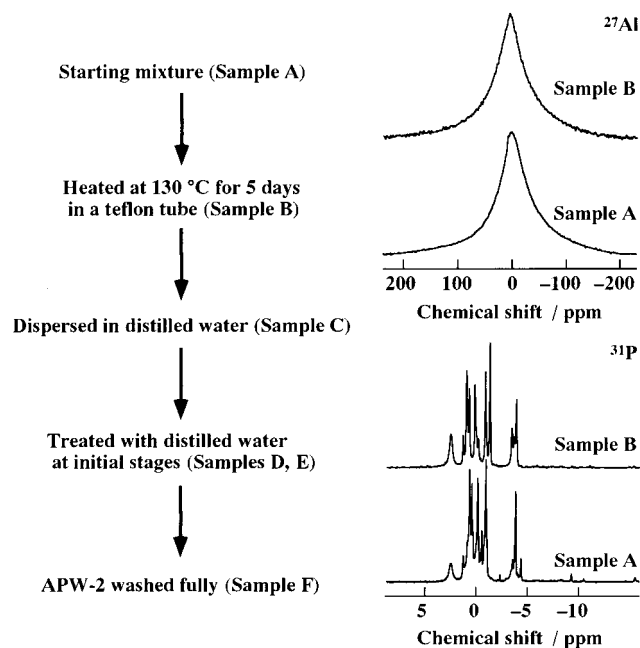


**Figure 10.** Scheme of the preparation of APW-2, and  $^{27}\text{Al}$  and  $^{31}\text{P}$  NMR spectra of the starting mixture and the resultant mixture after heating at 130 °C for 5 days.

starting mixture were changed at the same time, the various synthetic conditions were interrelated in this system.

### 3.4. Effect of Reaction Temperature and Time.

While holding the molar ratio of the starting mixture at 1:1:1:2:65/ $\text{Al}_2\text{O}_3$ : $\text{P}_2\text{O}_5$ : $\text{C}_{16}\text{TMACl}$ : $\text{TMAOH}$ : $\text{H}_2\text{O}$ , the reaction temperature and time were changed. Hexagonal mesostructured products were obtained in the range from room temperature to 130 °C, whereas lamellar mesostructured products formed at a higher temperature than 150 °C. With an increase in the reaction temperature, the progress of the condensation of inorganic species led to the formation of lamellar APW-1. In the same way, with an expanded reaction time, lamellar mesostructured products slightly increased even at 130 °C. These results support the conclusion that the extent of the condensation of inorganic species is important for the formation of APW-1 and APW-2. That is, it is necessary for the preparation of the APW-2 that the synthesis temperature should be lower in order to suppress the condensation of inorganic phases.

**4. Formation Process of APW-2.** The aforementioned syntheses were carried out at 130 °C and the variation in the synthetic conditions led to the formation of APW-1 in almost all cases because  $\text{C}_{16}\text{TMA}$  cations should assemble to balance the charge of frameworks composed of alternating  $\text{AlO}_4$  and  $\text{PO}_4$  units upon condensation. However, we noticed that APW-2 was obtained in a wider range under lower reaction temperatures because of a suppression of the condensation among inorganic species. This result indicates that a less condensed framework is necessary for the formation of APW-2. Therefore, we investigated the formation process of APW-2 by using the synthesis procedure shown in Figure 10 and then its unique framework was studied in more detail. We used the optimal conditions for the formation of APW-2. (The composition of the starting mixture was 1:1:1:2:65/ $\text{Al}_2\text{O}_3$ : $\text{P}_2\text{O}_5$ : $\text{C}_{16}\text{TMACl}$ : $\text{TMAOH}$ : $\text{H}_2\text{O}$ .)

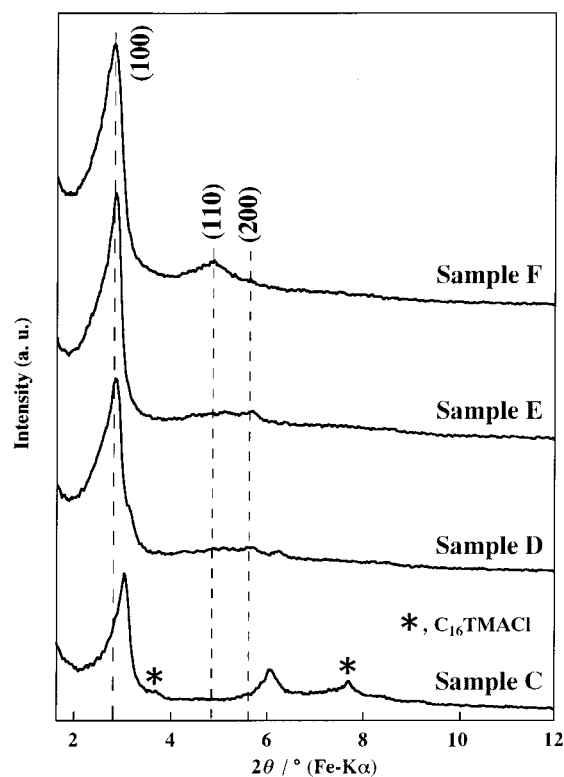


**Figure 11.** XRD patterns of the products obtained by the procedure of Figure 10.

A solid product was hardly obtained after heating at 130 °C for 5 days, although a slight amount of lamellar mesostructured product formed as a solid phase. The  $^{27}\text{Al}$  and  $^{31}\text{P}$  NMR spectra of the starting mixture (sample A) and the resultant one (sample B) after heating at 130 °C for 5 days are shown in Figure 10. Before and after the mixture was heated at 130 °C for 5 days, the  $^{27}\text{Al}$  NMR spectra of this mixture indicate the presence of octahedral Al species bonded to  $\text{HPO}_4^{2-}$  ions and the  $^{31}\text{P}$  NMR spectra showed many peaks mainly due to  $\text{HPO}_4^{2-}$  ions bonded to Al species except for the peak at 2.5 ppm due to  $\text{HPO}_4^{2-}$ .<sup>27</sup> This NMR result indicates that aluminophosphate oligomers are present in both samples A and B. However, the chemical shifts and the peak intensities in the  $^{31}\text{P}$  NMR spectrum were slightly changed before and after heating. This result suggests that both oligomerization and decomposition of aluminophosphate species coincide during the heating. Therefore, a solid product did not form at this stage.

When the resultant mixture was dispersed in distilled water, a white solid formed quickly. Because the pH value of the suspension was suddenly changed from  $\approx 10$  to  $\approx 8.5$ , the solubility of the resultant mixture probably becomes lower. It has been reported that an aluminophosphate gel forms in the medium pH range ( $2 < \text{pH} < 10$ ) with  $\text{Al/P} = 1$ .<sup>27a</sup> The XRD patterns of the solid products are shown in Figure 11. The XRD pattern of sample C indicates that the (200) peak was observed clearly. The  $d$ -spacing of the (100) peak became larger and the (110) and (200) peaks due to a hexagonal phase were gradually emphasized with an increase in the times of treatment with distilled water (samples D and E). The fully washed product (sample F) was assignable to a hexagonal phase.

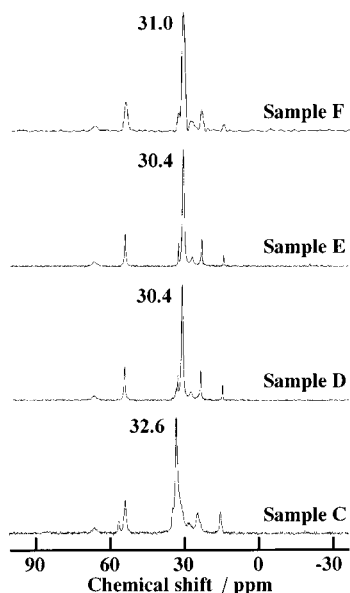


**Figure 12.**  $^{13}\text{C}$  CP/MAS NMR spectra of the products obtained by the procedure of Figure 10.

The  $^{13}\text{C}$  CP/MAS NMR spectra of samples C–F in Figure 12 showed signals due to the methylene groups of the  $\text{C}_{16}\text{TMA}$  cations at 32.6, 30.4, 30.4, and 31.0 ppm, respectively. The  $^{13}\text{C}$  CP/MAS NMR spectra of APW-1 and APW-2 showed the signals due to the methylene groups of the  $\text{C}_{16}\text{TMA}$  ions at 33.5 and 31.0 ppm, respectively. The chemical shift of sample C is in agreement with that of lamellar APW-1 and the chemical shifts of samples D–F agree with that of hexagonal APW-2.

These XRD and  $^{13}\text{C}$  CP/MAS NMR results indicate that a layered product (sample C) formed after the resultant mixture was dispersed in distilled water and the layered product gradually changes to hexagonal APW-2 (sample F).

When other compositions of the starting mixtures were used, the solid products obtained after heating at 130 °C for 5 days were lamellar APW-1 and the remaining liquid resultant mixtures converted to the layered products by dispersing in distilled water with the instant formation of solid products. The solid products changed to hexagonal APW-2 by repeated treatment with distilled water. Mixtures of APW-1 and APW-2 were obtained under various conditions by this process.

The  $^{27}\text{Al}$  and  $^{31}\text{P}$  MAS NMR spectra of sample C are shown in Figure 13. The  $^{27}\text{Al}$  MAS NMR spectrum showed mainly the presence of four-coordinated Al, being distinguished into two regions observed at 62.8 ppm and in the range from 45 to 38 ppm. The peak at 62.8 ppm can be assigned to  $\text{Al}(\text{OH})_4^-$  species bonded to  $\text{HPO}_4^{2-}$  ions<sup>27</sup> and the peaks at 44.3, 41.7, and 38.9 ppm show the existence of three kinds of  $\text{AlO}_4$  units, possibly due to  $\text{Al}(\text{OP})_{4-x}(\text{OH})_x$ .<sup>16</sup> The peak centered at  $-1.1$  ppm, being assignable to six-coordinated Al, may involve coordination with water molecules. At the next treatment (sample D), both four- and six-coordinated Al were detected as observed for APW-2 (Figure 3c).

The  $^{31}\text{P}$  MAS NMR spectrum of sample C showed several peaks at 1.4,  $-0.4$ ,  $-4.4$ ,  $-5.6$ ,  $-10.3$ ,  $-13.0$ , and  $-19.2$  ppm. The peak at 1.4 ppm is assignable to

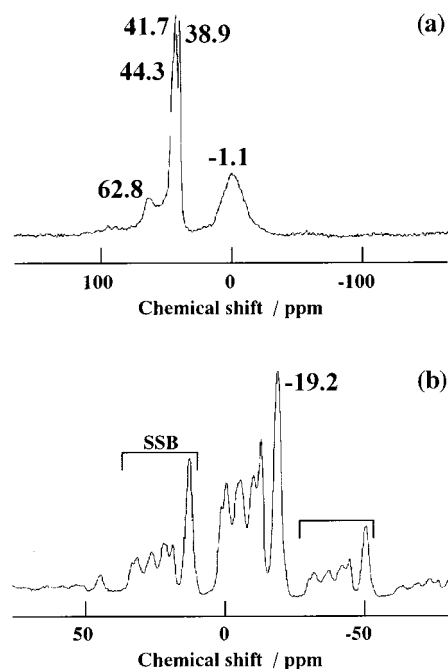


**Figure 13.** (a)  $^{27}\text{Al}$  and (b)  $^{31}\text{P}$  MAS NMR spectra of sample C.

**Table 2. Composition of Samples C–F**

sample	composition of organic fraction (mol %)		Al/P ratio	(Al+P)/N ratio
	$\text{C}_{16}\text{TMA}$	TMA		
C	65	35	1.11	2.7
D	97	3	1.20	3.3
E	100	0	1.20	3.8
F	100	0	1.49	4.0

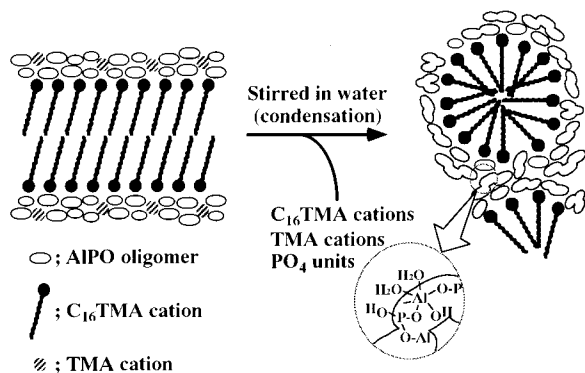
isolated  $\text{PO}_4$  units, the peaks from  $-0.4$  to  $-13.0$  ppm are assigned to  $\text{H}_3\text{PO}_4$  ligands around Al and  $\text{H}_2\text{PO}_4^-$  ligands around Al, and the peak at  $-19.2$  ppm is assignable to  $^-\text{OP}(\text{OAl})_3$  units.<sup>10,12,27</sup> These peaks can be attributed to an incompletely condensed framework. The peaks were observed in higher magnetic fields than those observed for sample B (Figure 10), meaning that insoluble aluminophosphate species were formed by sudden pH change described above.

The compositions of these products (samples C–F) are listed in Table 2. Both  $\text{C}_{16}\text{TMA}$  and TMA cations were present in sample C, a small amount of TMA ions were present in sample D, and no TMA cations were present in samples E and F. In addition, the (Al+P)/N and the Al/P ratio increased with the treatment times. From these results, in addition to the aforementioned roles of TMAOH, we suppose that both the  $\text{C}_{16}\text{TMA}$  and TMA cations interact with aluminophosphate oligomers and TMA cations suppress the polymerization of the aluminophosphate oligomers. Moreover, TMA cations are released in water at the beginning of the treatment with distilled water and  $\text{C}_{16}\text{TMA}$  cations were gradually dissolved in water until the fully washed sample was obtained. At the same time, isolated  $\text{PO}_4$  units and/or  $\text{PO}_4/\text{N}^+$  ion pairs may also be dissolved.

These results indicate that the formation mechanism of APW-2 can be described as shown in Scheme 1. A layered product composed of aluminophosphate oligomers and  $\text{C}_{16}\text{TMA}$  cations formed as an intermediate instantly after dispersing in distilled water. With an



### Scheme 1. Proposed Formation Mechanism of APW-2



increase in the times of treating with distilled water, the layered intermediate was transformed into hexagonal APW-2. Because aluminophosphate oligomers were precipitated at the time of dispersing in distilled water, APW-2 had the less condensed framework. The Al/P ratio ( $\approx 1.5$ ) of APW-2 results from the dissolution of isolated PO<sub>4</sub> units and/or PO<sub>4</sub>/N<sup>+</sup> ion pairs.

When C<sub>22</sub>TMA cations were used as a surfactant instead of C<sub>16</sub>TMA cations, lamellar mesostructured products were obtained under the same conditions. Even when the synthesis was carried out at room temperature, a hexagonal mesostructured product cannot be obtained. However, a hexagonal mesostructured product was obtained by using distilled water heated at 70 °C at the time of dispersing in distilled water followed by repeated washing.<sup>23</sup> These facts indicate that C<sub>22</sub>TMA cations were not likely to be excluded from a layer structure because C<sub>22</sub>TMA cations were almost insoluble in water. Therefore, the condensation of the framework proceeds without the structural change from a layer structure at room temperature. These results support the formation mechanism shown in Scheme 1.

## Discussion

**1. Structures of APW-1 and APW-2.** The precise crystal structure of lamellar APW-1 cannot be determined owing to the broad XRD peaks in the  $2\theta$  region above 15°. Therefore, we compare APW-1 with reported lamellar mesostructured aluminophosphates from the viewpoints of the coordination of Al and P atoms and the Al/P ratio in aluminophosphate frameworks. The framework of APW-1 was composed of alternating AlO<sub>4</sub> and PO<sub>4</sub> units and the Al/P ratio was 0.75. There have been several reports on lamellar aluminophosphates with Al/P ratios of 0.75.<sup>10,31</sup> These materials have alternating AlO<sub>4</sub> and PO<sub>4</sub> units. For a lamellar mesophase reported by Czarnetzki et al.,<sup>10</sup> the chemical shift of the Al atoms is 44.8 ppm and those of the P atoms are -8.4 and -16.2 ppm, being different from those observed for APW-1 (-17.1 and -20.3 ppm). Layered aluminophosphates reported by Jones et al.<sup>31</sup> have a

framework with a eight-membered ring or with a ten-membered ring of TO<sub>4</sub> units. The AFM image of APW-1 (not shown) showed a distorted hexagonal arrangement of TO<sub>4</sub> units, being different from the structures of layered aluminophosphates.<sup>31</sup>

The Al/P ratio of hexagonal APW-2 was 1.5 and the framework was less condensed. For hexagonal mesostructured and mesoporous aluminophosphates reported by Feng et al.,<sup>18</sup> Chakraborty et al.,<sup>19</sup> Holland et al.,<sup>21</sup> and Cheng et al.,<sup>22</sup> the Al/P ratio, the coordination of Al and P atoms in the frameworks, and the thermal stability are different from those observed for APW-2. For mesostructured and mesoporous aluminophosphates reported by Luan et al.,<sup>20c</sup> the <sup>27</sup>Al and <sup>31</sup>P MAS NMR spectra are similar to those observed for APW-2 and they claim that the materials are analogous to disordered mesoporous silicas such as KIT-1 and MSU-1. In contrast, the TEM image of APW-2 showed a relatively ordered hexagonal arrangement (Figure 2b) and APW-2 possesses higher thermal stability, up to 600 °C at the lowest.

In our experiment, the frameworks of APW-1 and APW-2 were clearly different, whereas the inorganic structures of the silicate-surfactant mesophases M41S are similar to that of silica gels with different extents of condensation.<sup>32,33</sup> This result can be explained in terms of the charge matching between the inorganic phases and surfactants.<sup>32,33</sup> For lamellar APW-1, the framework, Al<sub>3</sub>P<sub>4</sub>O<sub>16</sub><sup>3-</sup>, has negative charge, which needs three cations to balance the charge on the whole. Most of the <sup>-</sup>OP(OAl)<sub>3</sub> units were interacted with C<sub>16</sub>TMA cations and a small part of the units might interact with H<sup>+</sup>. For hexagonal APW-2, the charge of the framework is not clear at present. If hexagonal mesostructured AlPOs have three-dimensional networks composed of both Al(OP)<sub>4</sub> and P(OAl)<sub>4</sub> units as well as those of microporous AlPO<sub>4-n</sub> materials,<sup>1</sup> the framework has no charge. That is, cationic surfactants do not exist in hexagonal mesostructured AlPOs. Very recently, a lamellar mesostructured aluminophosphate with a more condensed framework, which was composed of Al(OP)<sub>4</sub>, <sup>-</sup>OP(OAl)<sub>3</sub>, and P(OAl)<sub>4</sub>, was reported.<sup>34,35</sup> However, mesostructured materials with completely condensed -Al-O-P- networks have never been reported up to now. For the synthesis of M41S materials,<sup>36</sup> no mesophases can be obtained at temperatures higher than 200 °C, even if the synthesis is performed using the same gel composition. The Q<sup>3</sup>/Q<sup>4</sup> ratio of the lamellar mesophase is larger than that of the hexagonal one,<sup>32,33</sup> so that more cationic surfactants are present in the lamellar mesophase. For APW-1 and APW-2, the C<sub>16</sub>TMA/(Al+P) values are 0.34 and 0.25, respectively. Moreover, the (Al+P)/N<sup>+</sup> ratios (Table 2) increased with the formation of APW-2. In this paper, we propose that

(31) (a) Jones, R. H.; Thomas, J. M.; Xu, R.; Huo, Q.; Cheetham, A. K.; Powell, A. V. *J. Chem. Soc., Chem. Commun.* **1991**, 1266-1268. (b) Thomas, J. M.; Jones, R. H.; Xu, R.; Chen, J.; Chippindale, A. M.; Natarajan, S.; Cheetham, A. K. *J. Chem. Soc., Chem. Commun.* **1992**, 929-931. (c) Chippindale, A. M.; Natarajan, S.; Thomas, J. M.; Jones, R. H. *J. Solid State Chem.* **1994**, *111*, 18-25. (d) Chippindale, A. M.; Clowley, A. R.; Huo, Q.; Jones, R. H.; Law, A. D.; Thomas, J. M.; Xu, R. *J. Chem. Soc., Dalton Trans.* **1997**, 2639-2643.

(32) (a) Huo, Q.; Leon, R.; Petroff, P. M.; Stucky, G. D. *Science* **1995**, *268*, 1324-1327. (b) Huo, Q.; Margolese, D. I.; Stucky, G. D. *Chem. Mater.* **1996**, *8*, 1147-1160.

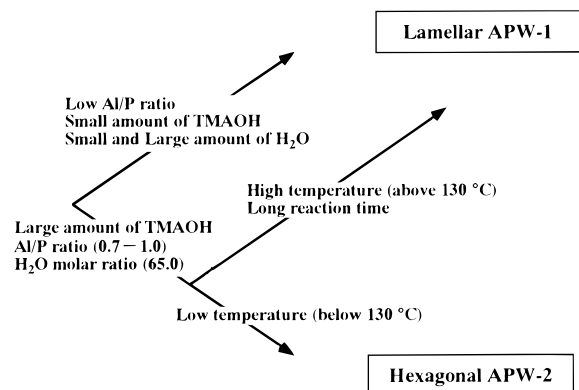
(33) Fyfe, C. A.; Fu, G. *J. Am. Chem. Soc.* **1995**, *117*, 9709-9714.

(34) Khimyak, Y. Z.; Klinowski, J. *J. Chem. Soc., Faraday Trans.* **1998**, *94*, 2241-2247.

(35) Khimyak, Y. Z.; Klinowski, J. *Chem. Mater.* **1998**, *10*, 2258-2265.

(36) Vartuli, J. C.; Schmitt, K. D.; Kresge, C. T.; Roth, W. J.; Leonowicz, M. E.; McCullen, S. B.; Hellring, S. D.; Beck, J. S.; Schlenker, J. L.; Olson, D. H.; Sheppard, E. W. *Chem. Mater.* **1994**, *6*, 2317-2326.

**Scheme 2. Effects of the Synthetic Conditions on the Structure of Mesostructured AIPOs Prepared Using ATMA Cations as Surfactants**



the charge balance in APW-2 is probably satisfied in its less condensed framework.

The charge of the inorganic phases in M41S materials gradually decrease as a result of the condensation of the silicate frameworks. In contrast, the charge is generally very high when  $-Al-O-P-$  networks with layered structures form; three negative charges are generated over seven or less  $TO_4$  units.<sup>31,37-39</sup> A structural change like that of the M41S materials is difficult for mesostructured AIPOs and this is the most important conclusion for the preparation of mesostructured AIPOs.

**2. Effects of the Synthetic Conditions.** Various synthetic conditions such as the amount of TMAOH, the amount of water, and the Al/P ratio are interrelated; the pH values, which affects the solubility of inorganic phases, change by alteration of the composition of the starting mixtures at the same time. The formation conditions of APW-1 and APW-2 are shown in Scheme 2. It is very important that the optimal composition of the starting mixtures should be selected for the formation of hexagonal APW-2. APW-1 is likely to form because of the presence of four-coordinated Al species at higher reaction temperatures which lead to the formation of  $-Al-O-P-$  linkages followed by the formation of  $Al_3P_4O_{16}^{3-}$  frameworks. Doping of a small amount of  $SiO_4$  units and the use of longer alkyl chain surfactants direct the formation of APW-1. No mesostructured products formed by changing the Al sources from  $Al(O^iPr)_3$  to  $AlCl_3 \cdot 6H_2O$ . The best way for the synthesis of APW-2 is to keep the reaction temperature lower than 130 °C in order to suppress condensation of aluminophosphate species in the starting mixtures. However, when longer alkyl chain surfactants are used, the temperature of the distilled water for both dispersing and treating should be higher because surfactants with longer alkyl chains do not dissolve very much in distilled water at room temperature.<sup>23</sup>

**3. Formation of APW-1 and APW-2.** APW-1 forms hydrothermally and APW-2 does not. At higher temperatures, APW-1 formed with the development of

aluminophosphate frameworks composed of both  $AlO_4$  and  $PO_4$  units. Our successful formation of APW-2 arises from controlling the extent of condensation of the inorganic phases. Interaction among the alkyl chains of  $C_{16}$ TMA cations is smaller than the covalent bond energy of the  $Al-O-P$  bonds, so that the formation of  $Al_3P_4O_{16}^{3-}$  frameworks is more critical for the formation of the specific mesostructures in this aluminophosphate- $C_{16}$ TMA system.

Nevertheless, the assemblies of  $C_{16}$ TMA cations are necessary for the synthesis of APW-1 and APW-2 because the assemblies direct the structures of the mesophases.<sup>5</sup> Sayari et al. applied the liquid-crystal templating (LCT) mechanism to the formation of mesostructured aluminophosphates using alkylamines; however, this consideration was used only for lamellar mesostructured aluminophosphates.<sup>14</sup> In their later review for non-silica periodic mesostructured materials,<sup>8</sup> they indicate that the lamellar mesophases using alkylamines do not have liquid-crystal phases. Before these reports, Oliver et al. proposed a supermolecular templating for the preparation of lamellar mesophases using alkylamines.<sup>13</sup> On the basis of both the LCT mechanism<sup>5</sup> and the packing parameter of surfactants reported by Huo et al.,<sup>32</sup> it is natural that mesostructured AIPOs with lamellar, hexagonal, and cubic structures can form because  $C_{16}$ TMA cations were used as the structure-directing agents as well as in the preparation of M41S materials.<sup>5</sup> Nevertheless, a cubic mesostructured AIPO cannot be obtained in our study. This fact is related to the formation mechanism in which APW-1 forms hydrothermally and APW-2 forms through a layered intermediate.

There have been several reports on the synthesis of hexagonal mesostructured materials from layered inorganic-surfactant intermediates.<sup>4,21,22,33,40-42</sup> After the discovery of the mesoporous silica derived from kanemite by Yanagisawa et al.,<sup>4</sup> Chen et al. show that hexagonal mesophase silicates derived from kanemite form by the transformation of a layered complex composed of fragments of silicate sheets and  $C_{16}$ TMA cations.<sup>42</sup> During this structural change, the amount of  $C_{16}$ TMA cations decrease. Fyfe et al. reported a phase transition from a layered complex, which composed of double-four-ring silicates  $Si_8O_{16}^{8-}$  and  $C_{16}$ TMA cations, to cubic MCM-48, to lamellar MCM-50, and to hexagonal MCM-41, in turn by acid treatment.<sup>33</sup> The  $Q^3/Q^4$  ratios of the products decrease by this transformation; therefore, the charge of the silicate frameworks also decreases. On the basis of both reports, the results obtained in this study are quite reasonable.

Hexagonal mesostructured aluminophosphates reported by Holland et al.<sup>21</sup> are prepared from layered complexes composed of Keggin-like  $Al_{13}$  cations and anionic surfactants; the material is mainly composed of  $AlO_6$  units. The hexagonal structure retains after heating in nitrogen at 200 °C for 1 h and is collapsed upon calcination even at 350 °C. The lower thermal stability is caused possibly by variation in the coordina-

(37) Kuperman, A.; Nadimi, A.; Oliver, S.; Ozin, G. A.; Garces, J. M.; Olken, M. M. *Nature* **1993**, *365*, 239-242.

(38) Tieli, W.; Long, Y.; Wenqin, P. *J. Solid State Chem.* **1990**, *89*, 392-395.

(39) Chippindale, A. M.; Powell, A. V.; Bull, L. M.; Jones, R. H.; Cheetham, A. K.; Thomas, J. M.; Xu, R. *J. Solid State Chem.* **1992**, *96*, 199-210.

(40) Inagaki, S.; Fukushima, Y.; Kuroda, K. *J. Chem. Soc., Chem. Commun.* **1993**, 680-682.

(41) Inagaki, S.; Koizumi, A.; Suzuki, N.; Fukushima, Y.; Kuroda, K. *Bull. Chem. Soc. Jpn.* **1996**, *69*, 1449-1457.

(42) Chen, C.-Y.; Xiao, S.-Q.; Davis, M. E. *Microporous Mater.* **1995**, *4*, 1-20.

tion of Al atoms upon calcination. Cheng et al.<sup>22</sup> have synthesized a layered kanemite-like aluminophosphate and the reaction of this material with C<sub>16</sub>TMA cations causes transformation to hexagonal mesostructured aluminophosphates as well as the reaction of kanemite with C<sub>16</sub>TMA cations.<sup>41,42</sup> However, the material is thermally unstable. Therefore, the hexagonal APW-2 reported here is very interesting not only in the formation process of the hexagonal mesostructured AlPOs but also because of its higher thermal stability (at the lowest 600 °C).

### Conclusions

Lamellar APW-1 has a regularity of  $-Al-O-P-$  bonds which affords a relatively condensed framework. Incomplete condensation of the inorganic phases was observed in hexagonal APW-2. The formation mechanism of APW-2 suggests that a layered precipitate, composed of aluminophosphate oligomers and C<sub>16</sub>TMA cations, transformed to hexagonal APW-2 with the

condensation of aluminophosphate oligomers. Only APW-2 is thermally stable and forms mesoporous aluminophosphates by calcination at 600 °C after substantial shrinkage of the framework. In the aluminophosphate-ATMA system, one of the most important factors is the charge balance between cationic surfactants and skeletal anionic charge depending on the  $-Al-O-P-$  framework. The formation process of APW-1 and APW-2 is applicable to the synthesis of novel non-silica-based mesostructured and mesoporous materials derived by the combination of two or more inorganic units.

**Acknowledgment.** The authors acknowledge Mr. M. Fuziwara, Materials Characterization Central Laboratory, Waseda University, for TEM measurements, and K. K. acknowledges financial assistance from a Grant-in-Aid for the Special Priority Area by the Ministry of Education, Science, and Culture of the Japanese Government.

CM981036H